

Process Integration of Supercritical CO₂ Cycle and Pumped Thermal Energy Storage (PTES) System

Junrong Tang^{a,b}, Qibin Li^{a,*}, Lina Wang^c, Haoshui Yu^{b,*}

^aKey Laboratory of Low-grade Energy Utilization Technologies and Systems, Ministry of Education, School of Energy and Power Engineering, Chongqing University, Chongqing, 400044, PR China

^bDepartment of Chemistry and Bioscience, Aalborg University, Niels Bohrs Vej 8A, Esbjerg, 6700, Denmark

^cSchool of Marine Technology and Environment, Dalian Ocean University, Dalian, China

qibinli@cqu.edu.cn; hayu@bio.aau.dk

This work introduces a novel energy system that combines the supercritical CO₂ (sCO₂) cycle with Pumped Thermal Energy Storage (PTES). This integration enhances efficiency, clean energy consumption, and storage capacity, effectively managing peak loads. While it uses extra electricity during off-peak hours for energy storage, it significantly boosts output during peak demand. The system offers flexibility with a load range of 92.49-103.59 % and a round-trip efficiency of 42.61 %. Parametric analysis indicates a trade-off between efficiency and power change rate, necessitating customization based on user needs.

1. Introduction

In recent years, the escalating energy demand, coupled with significant fossil fuel consumption and severe environmental repercussions, has posed one of the world's foremost challenges (Hoegh-Guldberg et al., 2019). Consensus has been reached on the crucial roles of widespread clean energy adoption and the development of efficient, low-to-zero carbon energy conversion systems in mitigating this crisis (Fankhauser et al., 2022). To achieve this goal, two primary strategies are generally employed: enhancing the efficiency of primary energy use and actively pursuing the development of new energy sources.

In terms of enhancing energy utilization efficiency, exploring new and efficient energy conversion technologies is a crucial step. Supercritical carbon dioxide (sCO₂) cycles have become a focal point in advanced energy conversion technologies due to their high efficiency and compact design (Guo et al., 2022). Feher (1968) proposed a notable seminal proposal of the sCO₂ Brayton cycle, which has offered critical insights for power system applications. To further enhance the efficiency of the sCO₂ cycle, Pérez-Pichel et al. (2012) explored the efficacy of integrated sCO₂/Organic Rankine cycle (ORC) systems, analyzing the placement of the ORC subsystem at four distinct locations. Tang et al. (2023) employed three types of Organic Flash Cycle (OFC) systems to integrate the combined sCO₂/OFCs systems, where detailed thermodynamic and exergoeconomic performance analyses were performed.

Other than enhancing energy utilization efficiency, renewable energy is another way to combat climate change. However, the inherently intermittent nature of primary renewable energy sources presents significant challenges for their integration into existing energy systems. Pumped Thermal Energy Storage (PTES) systems offer a novel approach to storing energy by using electricity to drive a heat pump that moves heat from a cold to a hot thermal reservoir (Benato and Stoppato, 2018). During periods of excess electricity generation, energy is stored thermally by a heat pump. When electricity is needed, the stored heat is converted back to electrical energy via a heat engine. To improve the system performance of PTES, researchers explored the incorporation of waste heat or low-grade heat sources with heat pumps during the charging process. This approach has led to the development of what is termed "thermally integrated PTES" (TI-PTES) (Frate et al., 2017). Hu et al. (2021) analyzed the TI-PTES system performance from the thermodynamic and economic viewpoints. They suggested that the integration of an additional low-grade heat source can increase the coefficient of performance (COP) of the heat pump and significantly improve the storage efficiency. Wang et al. (2022) compared two different TI-PTES systems driven by geothermal water, one using the organic flash cycle (OFC-TIPTES) and the other one

using the organic Rankine cycle (ORC-TIPTES). The ORC-TIPTES shows better performance of that than the OFC-TIPTES. Recently, Miao et al. (2024) developed an effective TI-PTES system, which integrated the LNG cold energy into the ORC system. They reported that compared to the basic TI-PTES system, the proposed LNG-TIPTES can improve the round-trip efficiency by 2.3 to 4.5 times higher.

Integrating renewable energy into the grid introduces challenges to the flexibility of electrical power systems, especially when the $s\text{CO}_2$ cycle operates under partial or overload conditions. These conditions lead to mismatches in electricity demand and significant energy losses. To address these issues, integrating energy storage like TI-PTES becomes crucial. This integration helps buffer the variability of renewable energy sources, supports broader adoption, improves load management capabilities, and aligns with sustainable energy goals. Therefore, this paper proposes a combined $s\text{CO}_2$ cycle and TI-PTES system, utilizing low-grade waste heat from the $s\text{CO}_2$ cycle to power the TI-PTES heat pump. This approach offers high efficiency, enhanced clean energy utilization, and better peak load management. In the integrated system, surplus electricity can be consumed by the Heat pump of PTES to generate heat energy during the off-peak period, which is used to drive the heat engine of PTES during the peak period. It enables the $s\text{CO}_2$ cycle to be operated flexibly in a wider range of power generation regulation capacities.

2. System description and model

2.1 System description

Figure 1 shows the diagram of the proposed $s\text{CO}_2$ -TIPTES system. In the $s\text{CO}_2$ cycle, CO_2 is compressed by the main compressor (MC) to state point 2, then heated by the Low-Temperature Recuperator (LTR) to state point 3a. It mixes with high-pressure CO_2 from the re-compressor (RC) at state point 3b, resulting in state point 3. This CO_2 is further heated in the High-Temperature Recuperator (HTR) and by a heat source to state point 5, before powering the $s\text{CO}_2$ turbine connected to a generator. The turbine exhausts in the HTR and LTR, reaching state point 8 (80 - 150°C), and splits into two streams: one heats the TI-PTES system and cools to state point 1, while the other is recompressed to state point 3b.

The TI-PTES comprises two subsystems: the heat pump (HP) and the Organic Rankine cycle (ORC), functioning during the charging and discharging phases. During the valley period, the HP subsystem captures waste heat from the $s\text{CO}_2$ cycle, converting excess electrical energy into thermal energy. The steam is compressed and cooled in the condenser to a saturated liquid, then cycled back after expansion. During the peak period, the ORC subsystem's steam expands in the turbine, generating electricity, then cools and cycles back, absorbing heat from the hot tank and completing the process. In short, the $s\text{CO}_2$ cycle operates all the time regardless of the off-peak/peak time. The $s\text{CO}_2$ cycle could run alone, at this time valve 1 (V1) is closed and valve 2 (V2) is open.

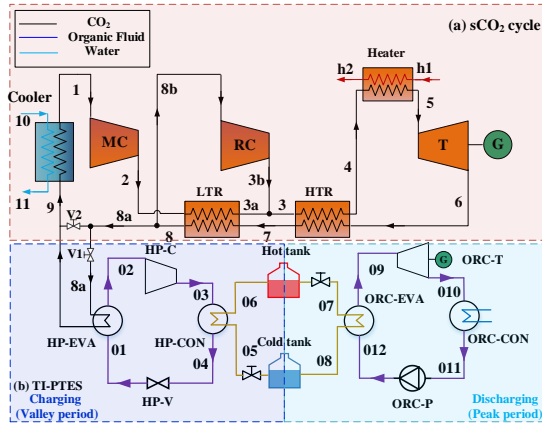


Figure 1: The layout of the integrated $s\text{CO}_2$ -TIPTES system.

2.2 System model

2.2.1 Mathematical model

The following appropriate assumptions are adopted to simplify the simulation (Li and Wang, 2019; Wu et al., 2020):

- (1) The analysis of system performance is analyzed under the assumption of steady-state operation.
- (2) It is assumed that all tanks are well-insulated, with negligible pressure, temperature, and heat losses.
- (3) It is presumed that there are no pressure drops or heat losses in the heat exchangers and pipelines.
- (4) The throttle valve is an isenthalpic process.

(5) The pinch point temperature difference (PPTD=10 °C) model is adopted for the HTR and LTR. For the proposed sCO₂/TI-PTES systems, the thermodynamic models can be developed based on the law of energy and mass conservation,

$$\sum \dot{m}_{in} = \sum \dot{m}_{out} \quad (1)$$

$$\sum \dot{Q} - \sum \dot{W} = \sum (\dot{m}h)_{out} - \sum (\dot{m}h)_{in} \quad (2)$$

where \dot{m} , \dot{Q} and \dot{W} denote the mass flow rate, heat transfer rate and work in each component. h is the specific enthalpy. Table 1 lists the detailed energy balance relations for the sCO₂/TI-PTES system.

Table 1 Energy and exergy destruction relations for the sCO₂/TI-PTES system.

Component	Energy balance relations	Component	Energy balance relations
Heater	$\dot{Q}_{heater} = \dot{m}_{CO_2}(h_4 - h_5)$	HP-EVA	$\dot{Q}_{HP-EVA} = \dot{m}_{CO_2}(1-x)(h_{8a} - h_9)$ $= \dot{m}_{01}(h_{02} - h_{01})$
Turbine	$\dot{W}_{tur} = \dot{m}_{CO_2}(h_5 - h_6)$	HP-C	$\dot{W}_{HP-C} = \dot{m}_{02}(h_{03} - h_{02})$
HTR	$\dot{Q}_{HTR} = \dot{m}_{CO_2}(h_4 - h_3) = \dot{m}_{CO_2}(h_6 - h_7)$	HP-CON	$\dot{Q}_{HP-CON} = \dot{m}_{03}(h_{03} - h_{04}) = \dot{m}_{05}(h_{06} - h_{05})$
LTR	$\dot{Q}_{LTR} = \dot{m}_{CO_2}(1-x)(h_3 - h_2) = \dot{m}_{CO_2}(h_7 - h_8)$	HP-V	$h_{01} = h_{04}$
MC	$\dot{W}_{MC} = \dot{m}_{CO_2}(1-x)(h_{2f} - h_1)$	ORC-EVA	$\dot{Q}_{ORC-EVA} = \dot{m}_{07}(h_{07} - h_{08})$ $= \dot{m}_{012}(h_{09} - h_{012})$
RC	$\dot{W}_{RC} = \dot{m}_{CO_2}x(h_{3b} - h_{8b})$	ORC-T	$\dot{W}_{ORC-T} = \dot{m}_{09}(h_{09} - h_{010})$
Pre-cooler	$\dot{Q}_{pc} = \dot{m}_{CO_2}(1-x)(h_9 - h_4) = \dot{m}_{cs}(h_{11} - h_{10})$	ORC-CON	$\dot{Q}_{ORC-CON} = \dot{m}_{010}(h_{010} - h_{011})$
		ORC-P	$\dot{W}_{ORC-P} = \dot{m}_{011}(h_{012} - h_{011})$

2.2.2 System Performance Criteria

For the proposed system, the round-trip efficiency (RTE) of the overall system can be defined as follows,

$$RTE = \frac{\int_0^{t_{char}} (W_T - W_{MC} - W_{RC} - W_{HP-C}) dt + \int_0^{t_{dischar}} (W_T - W_{MC} - W_{RC} + W_{ORC-T} - W_{ORC-P}) dt}{\int_0^{t_{char}} \dot{Q}_{heater} dt + \int_0^{t_{dischar}} \dot{Q}_{heater} dt} \times 100\% \quad (3)$$

where t_{char} and $t_{dischar}$ refer to the time of charging and discharging.

In addition, to evaluate the peak shaving capability of the TI-PTES to the sCO₂ power generation system, the power change rate (PCR) is selected and can be expressed as follows (Lu et al., 2024),

$$PCR = \frac{(\dot{W}_{net,sCO_2} + \dot{W}_{net,ORC-T}) - (\dot{W}_{net,sCO_2} - \dot{W}_{HP-C})}{\dot{W}_{net,sCO_2}} \times 100\% \quad (4)$$

3. Results and discussion

3.1 Basic case analysis

This section displays the system performance under the basic design conditions. The thermophysical properties of the working fluids are obtained from REFPROP (Lemmon et al., 2018). And simulations are conducted in MATLAB software. Noted that as a promising fluid for PTES, R1233zd(E) is used as the working fluid (Miao et al., 2024; Wang et al., 2023). The basic operating conditions of the proposed system are listed in Table 2.

Table 2. The basic input values for simulation (Miao et al., 2024; Wang et al., 2022; Wang and Dai, 2016).

Subsystem	Parameters	Value	Subsystem	Parameters	Value
sCO ₂ cycle	Ambient temperature /°C	25	TI-PTES	Hot tank temperature /°C	120
	Ambient pressure /kPa	101.325		cold tank temperature /°C	60
	Main compressor inlet pressure /MPa	7.4		Evaporation temperature of HP /°C	80
	Turbine inlet pressure /MPa	25		Pinch point of heat exchanger /°C	5
	Main compressor inlet temperature /°C	32		Superheat degree of evaporator /°C	4
	Heat source temperature /°C	800		Compressor efficiency /%	80
	Turbine inlet temperature /°C	550		Pump isentropic efficiency /%	70
	Turbine isentropic efficiency /%	90		Turbine isentropic efficiency /%	80
	Compressor isentropic efficiency /%	85		Storage time /h	6
	Flow split ratio (x)	0.3		Working fluid	R1233zd(E)
	Rated power (MW)	50			

Table 3 compares the thermodynamic performance of the sCO₂/TI-PTES system with a standalone sCO₂ system. During off-peak hours, the sCO₂ cycle operates normally while the TI-PTES heat pump converts sCO₂ waste heat into high-temperature energy stored in pressurized water. This process consumes an extra 3.75 MW of electricity, lowering the system's output and reducing electrical efficiency to 40.20 % during charging, a

decrease of 3.26 % from the standalone system. In peak periods, the sCO₂ system functions typically, but the TI-PTES system uses stored heat to power the ORC subsystem, producing an extra 1.79 MW of electricity. This increases the discharging phase efficiency to 45.02 %, 1.56 % higher than the standalone system. Overall, the round-trip efficiency is 42.61 %, with the sCO₂/TI-PTES system offering better flexibility, a PCR of 11.09 %, and a load range of 92.49 %-103.59 %.

Table 3. System performance comparison between the proposed system and stand-alone sCO₂ system.

Parameters	Valley period		Peak period	
	sCO ₂ /TI-PTES	sCO ₂	sCO ₂ /TI-PTES	sCO ₂
Power generation by sCO ₂ cycle (MW)	50	50	50	50
Storage power of TI-PTES (MW)	3.75	/	1.79	/
Net power output of the overall system (MW)	46.25	50	51.79	50
System power efficiency (%)	40.20	43.46	45.02	43.46

3.2 Parameter analysis

In the parameter analysis, four decision-making parameters have been chosen: split ratio of sCO₂ cycle, the evaporation temperature of HP and the temperature of hot and cold tanks. The first parameter significantly influences the sCO₂ cycle system performance, while the remaining three parameters are crucial for the power storage capacity of PTES system. During the parametric analysis of each parameter, the other parameters remain the same as the basic conditions.

3.2.1 Effect of split ratio of sCO₂ cycle

Figure 2 illustrates the impact of the split ratio in the sCO₂ cycle on system performance. It is observed that there is an optimal split ratio ($x=0.29$) at which the RTE is maximized, while the PCR reaches its minimum value. This phenomenon occurs because, as the split ratio increases, the heat available to the TI-PTES system from the sCO₂ cycle initially decreases before increasing, mirroring the trend in power consumption and output during the charging and discharging processes of the PTES system, as shown in Figure 2(a).

When x is below 0.29, the rate of decrease in power consumption by the heat pump cycle's compressor is significantly greater than the net power output of the ORC cycle, leading to an upward trend in system efficiency. Conversely, when the split ratio exceeds 0.29, the power consumption by the compressor substantially increases at a rate greater than the net power output by the ORC, causing a decline in efficiency. The PCR value directly depends on the PTES system's power input during charging and output during discharging. Consequently, PCR exhibits a trend similar to that of the corresponding power changes.

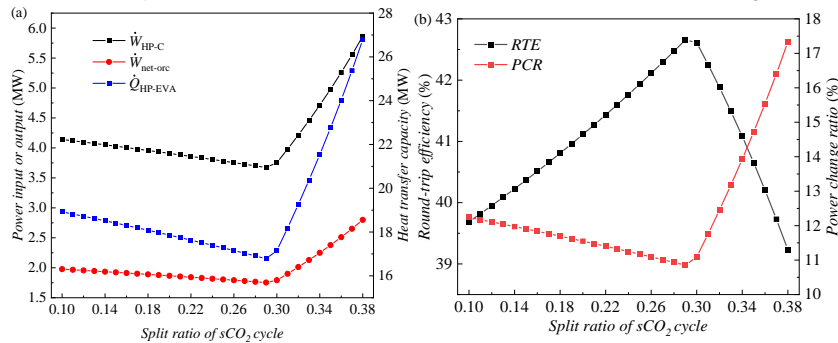


Figure 2: Effect of the split ratio of sCO₂ cycle on system performance.

3.2.2 Effect of evaporation temperature of HP

Figure 3 demonstrates the impact of the HP evaporator temperature on system performance. It is observed that as the evaporator temperature increases, the RTE and PCR exhibit opposite trends: RTE increases with rising temperature, while PCR does the opposite. The reason for these trends is that an increase in evaporator temperature implies a reduction in the heat input to the TI-PTES system, which leads to a decrease in the flow rate of the TI-PTES subsystem. Consequently, this results in a reduction in both the power consumption of the heat pump's compressor and the power output of the ORC system. This reduction in power consumption and output naturally leads to a decrease in PCR. Regarding RTE, the rate of decrease in compressor power

consumption is significantly greater than the rate of decrease in the net output rate of the ORC system. Therefore, RTE exhibits an increasing trend.

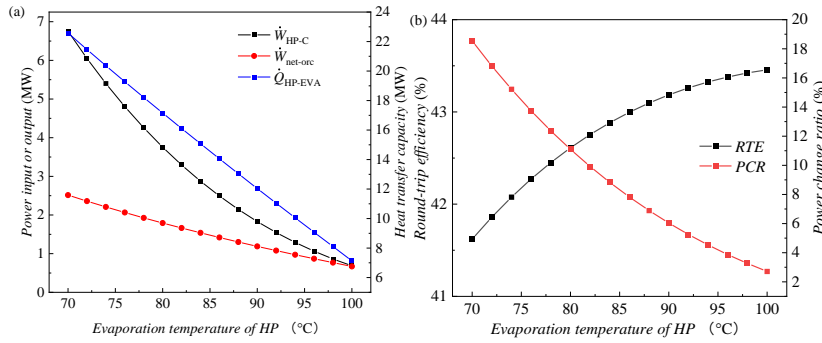


Figure 3: The effect of evaporation temperature of HP on system performance.

3.2.3 Effect of the temperature of hot and cold tanks

Figure 4 illustrates the comprehensive impact of the cold and hot storage tank temperatures of the TI-PTES system on system performance. It is observed from Figures 4(a) and (b) that RTE and PCR exhibit opposing trends as well. When RTE is high, the corresponding PCR is low, and the reasons are similar to those described for the previous parameters. Concerning individual parameters, it is noted that a higher cold tank temperature is beneficial for both the system's RTE and PCR. In terms of the hot tank temperature, it is evident that under a fixed cold tank temperature, a lower hot tank temperature contributes to achieving a higher RTE. Conversely, to attain a higher PCR, a higher hot tank temperature is required.

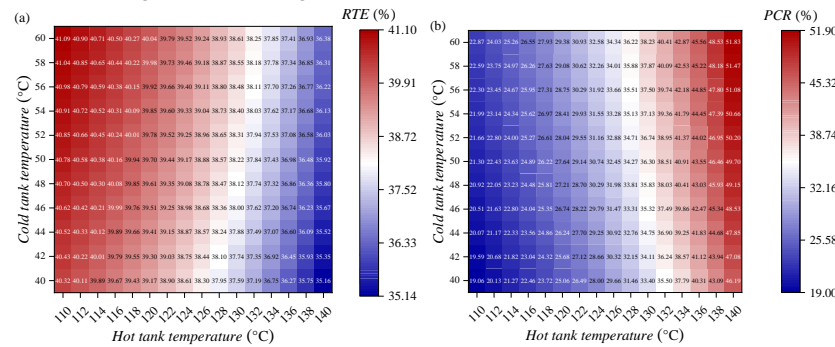


Figure 4: The effect of evaporation temperature of HP on system performance

4. Conclusions

The integration of TI-PTES with the sCO_2 system presents a promising approach to developing more efficient energy systems. The combined sCO_2 /TI-PTES system enhances discharging efficiency by up to 45.02 %, provides greater system flexibility, and supports a broader load range (92.49 %-103.59 %). These features showcase its potential to bolster grid stability and facilitate the integration of renewable energy sources. Notably, the system achieves maximum RTE at a split ratio of 0.29, although at this point, the PCR is at its minimum value. Additionally, variations in evaporation temperature and the temperatures of the hot and cold storage tanks impact both RTE and PCR, underscoring the need for careful system design to optimize overall performance. By addressing these factors, this work highlights the importance of the combined sCO_2 and TI-PTES system in enhancing clean energy utilization, improving peak load management, and supporting the broader adoption of renewable energy sources.

Despite the advantages, the proposed system has some weaknesses that must be considered. The complexity of integrating the sCO_2 and TI-PTES systems requires meticulous system design and optimization, particularly concerning the split ratio, to effectively balance efficiency and power conversion. Initial investment costs for such an integrated system can be substantial, posing a barrier to widespread adoption.

Nomenclature

0 – dead (ambient) state
 Q – heat transfer rate, MW

RTE – round-trip efficiency, %
 PTES – pumped thermal energy storage

PCR – power change rate, %

P – pressure, MPa

v – valve

T – temperature, °C

sCO₂ – supercritical carbon dioxide

1,2,etc – state points

\dot{W} – power/work, MW

x – split ratio

s – entropy, kJ/(kg ·K)

η – efficiency, %

Acknowledgments

Dr. Junrong Tang is grateful for the financial support from the China Scholarship Council (CSC NO.202206050138).

References

- Benato A., Stoppato A., 2018. Pumped Thermal Electricity Storage: A technology overview. *Thermal Science and Engineering Progress*, 6, 301-315.
- Fankhauser S., Smith S.M., Allen M., Axelsson K., Hale T., Hepburn C., Kendall J.M., Khosla R., Lezaun J., Mitchell-Larson E., Obersteiner M., Rajamani L., Rickaby R., Seddon N., Wetzler T., 2022. The meaning of net zero and how to get it right. *Nature Climate Change*, 12(1), 15-21.
- Feher E.G., 1968. The supercritical thermodynamic power cycle. *Energy Conversion*, 8(2), 85-90.
- Frate G.F., Antonelli M., Desideri U., 2017. A novel Pumped Thermal Electricity Storage (PTES) system with thermal integration. *Applied Thermal Engineering*, 121, 1051-1058.
- Guo J.-Q., Li M.-J., He Y.-L., Jiang T., Ma T., Xu J.-L., Cao F., 2022. A systematic review of supercritical carbon dioxide (S-CO₂) power cycle for energy industries: Technologies, key issues, and potential prospects. *Energy Conversion and Management*, 258, 115437.
- Hoegh-Guldberg O., Jacob D., Taylor M., Guillén Bolaños T., Bindi M., Brown S., Camilloni I.A., Diedhiou A., Djalante R., Ebi K., 2019. The human imperative of stabilizing global climate change at 1.5 °C. *Science* 365(6459), eaaw6974.
- Hu S., Yang Z., Li J., Duan Y., 2021. Thermo-economic analysis of the pumped thermal energy storage with thermal integration in different application scenarios. *Energy Conversion and Management* 236, 114072.
- Lemmon E., Bell I.H., Huber M., McLinden M., 2018. NIST Standard Reference Database 23: Reference Fluid Thermodynamic and Transport Properties-REFPROP, Version 10.0, National Institute of Standards and Technology. Standard Reference Data Program, Gaithersburg, United States, <https://tsapps.nist.gov/publication/get_pdf.cfm?pub_id=912382>, accessed 03.07.2024.
- Li B., Wang S.S., 2019. Thermo-economic analysis and optimization of a novel carbon dioxide based combined cooling and power system. *Energy Conversion and Management*, 199, 112048.
- Lu M., Du Y., Yang C., Zhang Z., Wang H., Sun S., 2024. Performance analysis and multi-objective optimization of a combined system of Brayton cycle and compression energy storage based on supercritical carbon dioxide. *Applied Thermal Engineering*, 236, 121837.
- Miao Z., Zhang M., Yan P., Xiao M., Xu J., 2024. Thermodynamic analysis of a low-temperature Carnot battery promoted by the LNG cold energy. *Journal of Energy Storage*, 88, 111619.
- Pérez-Pichel G.D., Linares J., Herranz L., Moratilla B.Y., 2012. Thermal analysis of supercritical CO₂ power cycles: Assessment of their suitability to the forthcoming sodium fast reactors. *Nuclear Engineering and Design*, 250, 23-34.
- Tang J.R., Li Q.B., Wang S.K., Yu H.S., 2023. Thermo-economic optimization and comparative analysis of different organic flash cycles for the supercritical CO₂ recompression Brayton cycle waste heat recovery. *Energy*, 278, 128002.
- Wang P., Li Q., Liu C., Wang R., Luo Z., Zou P., Wang S., 2022. Comparative analysis of system performance of thermally integrated pumped thermal energy storage systems based on organic flash cycle and organic Rankine cycle. *Energy Conversion and Management*, 273, 116416.
- Wang P., Li Q., Wang S., He C., Tang J., 2023. Thermo-economic analysis and comparative study of different thermally integrated pumped thermal electricity storage systems. *Renewable Energy*, 217, 119150.
- Wang X.R., Dai Y.P., 2016. Exergoeconomic analysis of utilizing the transcritical CO₂ cycle and the ORC for a recompression supercritical CO₂ cycle waste heat recovery: A comparative study. *Applied Energy*, 170, 193-207.
- Wu C., Xu X.X., Li Q.B., Li J., Wang S.S., Liu C., 2020. Proposal and assessment of a combined cooling and power system based on the regenerative supercritical carbon dioxide Brayton cycle integrated with an absorption refrigeration cycle for engine waste heat recovery. *Energy Conversion and Management*, 207, 112527.